Kinetics of the simultaneous syntheses of ethyl *tert*-butyl ether (ETBE) and butyl *tert*-butyl ether (BTBE) over Amberlyst™ 35

Jordi H. Badia*, Carles Fité, Roger Bringué, Fidel Cunill, Javier Tejero

Departament d'Enginyeria Química i Química Analítica, Facultat de Química, Universitat de Barcelona (UB), C. de Martí i Franquès 1-11, 08028 Barcelona (Spain)

*Corresponding author. Tel.: +34 93 402 1288. E-mail address: jhbadia@ub.edu

ABSTRACT

The kinetics of the simultaneous syntheses of ethyl *tert*-butyl ether (ETBE) and butyl *tert*-butyl ether (BTBE) over Amberlyst™ 35 (A35) has been studied at 315–353 K in the liquid phase. Different kinetic modeling approaches—namely, empirical power-law modeling, mechanistic modeling based on Langmuir-Hinshelwood-Hougen-Watson (LHHW) and Eley-Rideal (ER) formalisms, and information-based modeling—have been compared. Empirical kinetic equations yield optimal quality of the fit, whereas mechanistic equations can explain the mechanisms of the studied reactions. The best mechanistic equation for both reactions corresponds to an ER-type mechanism in which an alcohol molecule (ethanol or 1-butanol) is adsorbed on one active site and reacts with isobutene from solution to produce the corresponding adsorbed ether molecule (ETBE or BTBE), which desorbs. A model built based on previous data has been used to check the validity of the inferred mechanism, while significantly reducing the number of adjustable parameters in the model.

KEYWORDS

Kinetics; etherification; isobutene; ethanol; 1-butanol; Amberlyst™ 35

1. INTRODUCTION

Liquid-phase etherification of 2-methylpropene (isobutene) with alcohols to give branched ethers has been a major industrial process since the introduction of oxygenated octane enhancers in gasoline, after the phase out of lead-based additives by the end of the 20th century. Most known examples are methyl *tert*-butyl ether (MTBE) and ethyl *tert*-butyl ether (ETBE), obtained by reaction with methanol and ethanol, respectively, over an ion-exchange resin catalyst. Analogous ethers can be obtained from other alcohols, such as 1-propanol and 1-butanol, which are extensively produced at industrial scale by the oxo process [1], or by biomass-based production routes, namely, the condensation of bioethanol and/or biomethanol (Guerbet catalysis) and the ABE fermentation, which produces a mixture of acetone, 1-butanol and ethanol [2–5]. Provided that the designated alcohol is obtained from biomass, the corresponding ether is considered to contribute in accomplishing the biofuel target. Furthermore, promising catalytic routes for obtaining biomass-based isobutene are currently being investigated with different degrees of success, which reinforce the renewable character of these ethers [6–8]. Nowadays, these ethers are relevant in the framework of obtaining renewable chemicals for use as biofuels and/or biolubricants to substitute non-renewable, oil-based ones [9,10].

Butyl *tert*-butyl ether (BTBE) is obtained by reaction between isobutene and 1-butanol. The simultaneous production of ETBE and BTBE in the same reaction unit (Scheme 1), which was studied in a previous work [11], would allow feeding ethanol and 1-butanol from renewable sources (e.g., ABE fermentation) to current ETBE production facilities without further alcohols

separation. This process can be of interest for manufacturers since it brings versatility to adapt the production targets to the market demands and stock disposal. Preferential adsorption of ethanol over 1-butanol on the catalyst active sites was observed, which, ultimately, hindered BTBE formation rates [11]. Interestingly, BTBE formation rates are much faster than ETBE rates when both reactions proceed individually, which is consistent with the higher reactivity of larger primary alcohols with isobutene [12–15], but when both reactions take place simultaneously the opposite is observed [11].

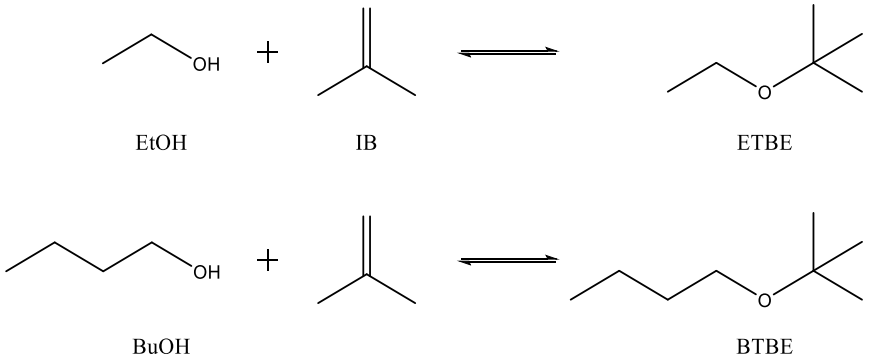

SCHEME 1. Studied reaction system.

The knowledge of the mechanism and thermodynamic limitation of both reactions is of utmost importance for setting the industrial operation conditions. In this regard, we detected a lack of literature references aimed at characterizing the kinetics of reaction systems where two chemical species compete for the same catalyst active sites. The aim of the present work is to study the kinetics of the simultaneous production of ETBE and BTBE over A35.

2. EXPERIMENTAL SECTION

2.1. CHEMICALS AND CATALYST

Reactants were ethanol (EtOH), 1-butanol (BuOH), and 2-methylpropene (IB). Some chemical standards were used for analytical procedures: 2-methyl-2-propanol (TBA), diethyl ether (DEE), 2,4,4-trimethyl-1-pentene (TMP-1), 2,4,4-trimethyl-2-pentene (TMP-2), 2-ethoxy-2-methylpropane (ETBE), and 1-*tert*-butoxybutane (BTBE). The source and purity of all compounds is listed in Table 1.

TABLE 1. Source, purity, and analysis of used materials.

Compound	Source	Mass fraction purity [%]	Analysis method
ethanol	Panreac	≥ 99.8	gas chromatography
1-butanol	Sigma-Aldrich	≥ 99.8	gas chromatography
2-methylpropene	Air Liquide	≥ 99.9	gas chromatography
2-methyl-2-propanol	Panreac	≥ 99.7	gas chromatography
diethyl ether	Panreac	≥ 99.5	gas chromatography
2,4,4-trimethyl-1-pentene	Sigma-Aldrich	≥ 98.0	gas chromatography
2,4,4-trimethyl-2-pentene	Sigma-Aldrich	≥ 98.0	gas chromatography
2-ethoxy-2-methylpropane	TCI Europe	≥ 95.0	gas chromatography
1-*tert*-butoxybutane	Synthesized and purified in our lab	≥ 98.0	gas chromatography
Nitrogen	Air Liquide	≥ 99.9995	–
Helium	Abelló-Linde	≥ 99.998	–
hydrogen	Air Liquide	>99.99	–
synthetic air	Air Liquide	>99.999	–

The ion-exchange resin Amberlyst™ 35 (A35) was used as the catalyst. A35 is a macroreticular, strongly acidic, sulfonated polymer of styrene-divinylbenzene. Its physical properties can be found elsewhere [16]. In a previous work, A35 showed the highest activity level with low byproducts formation among six acidic ion-exchange resins tested in the present reaction system [11].

2.2. EXPERIMENTAL SETUP AND PROCEDURE

Experiments were performed at a constant temperature, in the range 315–353 K and 2.5 MPa in a stirred tank batch reactor. The reactants composition was varied as follows: the initial ethanol/1--butanol molar ratio ($R°_{E/B}$) varied from 0.5 to 2.0, and the initial alcohols/isobutene molar ratio (that is, moles of both alcohols per mole of isobutene, $R°_{A/IB}$) varied from 0.5 to 5.5, with the total amount of reactants being always about 2.2–2.4 moles. These ranges of the initial compositions allowed covering for a wide range of global properties of the reactants mixture, which might affect the reaction mechanism including the behavior of the resin as a catalyst [12,13,17]. The total volume of the reactants mixture was approximately of 200 cm^3.

Before every experimental run, a drying protocol for the catalyst was applied. It consisted of three steps: firstly, the catalyst was dried at room temperature for 48 h, then introduced in an atmospheric oven at 383 K for 2.5 hours and, finally, placed in a vacuum oven at 373 K and 0.001 MPa for at least 12 h until the run started. By means of this procedure, the final water content in the resin beads was 3-5 wt.%, determined by Karl-Fischer titration in the lab.

Experiments were performed with catalyst beads that had been crushed and sieved to obtain particle sizes in the ranges of 0.25-0.40 mm and 0.08-0.16 mm. In a previous work, it was observed that particles below 0.40 mm showed no significant diffusional effects at 333 K for a wide variety of acidic ion-exchange resins in the syntheses of MTBE, ETBE, PTBE, and BTBE (by isobutene etherification with methanol, ethanol, 1-propanol, and 1-butanol, respectively) [18].

The experimental procedure consisted of the following: firstly, the catalyst (about 0.1 to 1.0 %wt. of the reactants mixture) was loaded into a catalyst injector and it was pressurized to 2.5 MPa with nitrogen. Then, the reactants were introduced separately into the reactor vessel: the alcohols were directly placed inside the reactor at atmospheric pressure and isobutene was introduced into the reactor from a pressure burette by pressure difference, impelled by nitrogen, up to a pressure of 1.0–1.5 MPa. The reactor stirring was switched on and the reaction mixture was heated until it reached the designated temperature (controlled within ± 0.1 K). The catalyst was injected into the vessel and the total pressure in the reactor was set at 2.5 MPa with nitrogen. This instant was considered as the starting point for the reaction. Each experimental run lasted about 5-8 h.

Samples were taken inline from the reaction medium approximately every 30 min with a sampling valve that injected 0.2 µL of pressurized liquid into an Agilent 6890 gas chromatograph attached to a mass selective detector HP5973N (GC-MS), which allowed to identify and quantify the reaction mixture components. The electron source of the mass detector was set to 503 K and the quadrupole to 423 K. The GC was equipped with a capillary column (HP-PONA 19091S-001, J&W Scientific, Santa Clara, US; 100% dimethylpolysiloxane, 50 m × 0.20 mm × 0.50 µm). Helium was the carrier gas, and its flowrate was set to 0.6 mL/min. The oven temperature was programmed with an initial 10 min hold at 333 K followed by a 10 K/min ramp, up to 353 K, and a second hold of 11.5 min at 353 K.

2.3. CALCULATIONS

Reaction rates were estimated from the slope of the empirical function fitted to the measured mole evolution, as follows:

$$r_j = \frac{1}{W_{\text{cat}}}\left(\frac{dn_j}{dt}\right) \tag{1}$$

where W_{cat} is the weight of the dry catalyst, n_j is the number of moles of the compound j and t is the time of reaction. More details regarding the calculation of experimental reaction rates are provided in Section S1 of Appendix A. Supplementary material.

For each considered kinetic equation, the optimal parameter values were obtained by minimization, using the Levenberg-Marquardt algorithm, of the total weighted sum of residual squares (*TWSRS*), defined as follows:

$$TWSRS = \sum_{i=1}^{r} \frac{1}{\left(r_{i,\,\max}^{\exp}\right)^2} \cdot SRS_i = \sum_{i=1}^{r} \frac{\left(r_i^{\exp} - r_i^{\text{calc}}\right)^2}{\left(r_{i,\,\max}^{\exp}\right)^2} \tag{2}$$

where $r_i^{\exp}$ is the experimental reaction rate of reaction i, r_i^{calc} is the calculated one from the model, and the weight factor, $1/\left(r_{i,\,\max}^{\exp}\right)^2$, allows normalizing the objective functions between zero and one. By normalizing the objective functions, the same importance is given to all responses and, therefore, biases due to the different magnitudes of the experimental reaction rates are avoided [19].

The fitted kinetic equations were ranked from higher to lower likelihood through the estimator Δ_S, which provides information regarding the empirical support of model S (the lowest Δ_S value signaling the most plausible equation), and is defined as follows [20,21]:

$$\Delta_S = AICc_S - AICc_{min} \tag{3}$$

where *AICc* is the bias-corrected reduced Akaike Information Criterion (*AIC*) for relatively small samples [20,21]:

$$AICc = AIC + \frac{2k(k+1)}{m-k-1} \tag{4}$$

$$AIC = m\left[ln\left(\frac{TWSRS}{m}\right)\right] + 2k \tag{5}$$

Parameters m and k in Equations 4 and 5 correspond, respectively, to the number of experimental points and the number of parameters in the fitted equation. When $m/k < 40$, it is advisable to use *AICc* instead of AIC [20,21].

Akaike weights, w, allow measuring the probability that each model is the actual best model among the R candidate ones, given the available dataset. Akaike weights can be calculated as follows:

$$w_S = \frac{exp\left(-\Delta_S/2\right)}{\sum_{r=1}^{R} exp\left(-\Delta_S/2\right)} \tag{6}$$

3. RESULTS AND DISCUSSION

3.1. EXPERIMENTAL RESULTS

Figure 1 shows the initial reaction rate dependence on the temperature (a), on the isobutene content in the reaction mixture (b), and on the alcohols concentration (c). As seen in Figure 1a, reaction rates obtained with 0.25-0.40 mm catalyst beads at the highest assayed temperature (353 K) are lower than expected, which suggests transport limitations arising at the highest assayed temperature. Additional experiments were carried out using 0.08-0.16 mm catalyst beads at a close temperature (shown as open symbols in Figure 1a) that yielded well-aligned reaction rate, which consequently can be considered as free from mass transfer limitations. Henceforward, only reaction rates free from mass transfer effects are considered for the kinetic analysis.

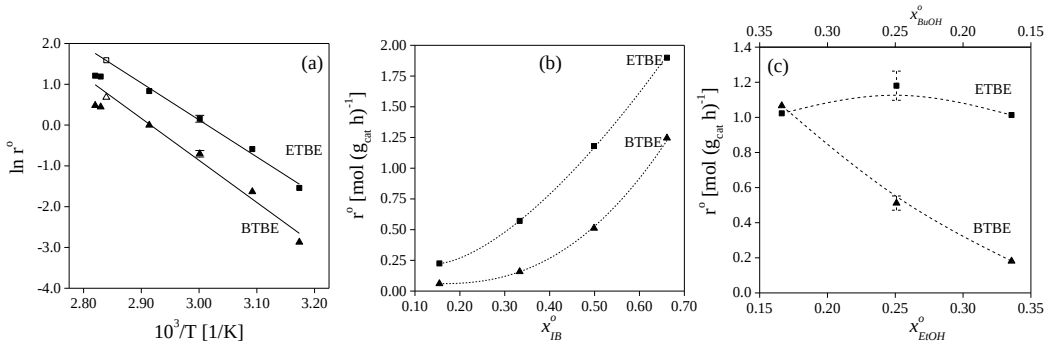

FIGURE 1. Arrhenius plot of initial reaction rate data at $R°_{A/IB}$ = 1.0 (a), initial etherification rates as a function of the initial isobutene molar fraction at T = 333 K and $R°_{E/B}$ = 1.0 (b), and initial reaction rates as a function of the initial alcohols molar fraction at T = 333 K and $R°_{A/IB}$ = 1.0 (c). Solid symbols: initial formation rates of ETBE (■) and BTBE (▲) using 0.25-0.40 mm catalyst beads. Open symbols: initial formation rates of ETBE (□) and BTBE (△) using 0.08-0.16 mm catalyst beads. Error bars are referred to standard error for replicated experiments. Solid lines represent the fit of rate data to straight lines. Dashed lines are guides to the eye.

The apparent activation energy for each synthesis reaction can be estimated from the slope of the straight lines in Figure 1a: (75 ± 4) kJ mol^{-1} for the ETBE reaction formation and (86 ± 6) kJ mol^{-1} for BTBE. These values are close to those quoted in literature for similar reaction systems over the same catalyst, typically in the range 67-84 kJ/mol [16,19,22–24].

The initial formation rates of both ethers increases with temperature and with the initial amount of isobutene (Figure 1b), as discussed elsewhere [11]. BTBE initial formation rate drops drastically as the initial amount of 1-butanol diminishes, whereas ETBE rates are hardly affected by the alcohols concentration in the reactants mixture (Figure 1c). This fact suggests preferential adsorption of ethanol over 1-butanol over the catalyst active sites.

3.2. EMPIRICAL FIT OF KINETIC DATA

As a first approach to model the kinetics of somewhat complex reaction systems, empirical fitting of kinetic data based on a power-law model can be carried out. This approach is often found useful for process simulators implementation and to quickly obtain expressions able to predict reaction rates within a certain range of operating conditions. As inferred from Figure 1, initial rate data are expected to be influenced by, at least, the following variables: temperature and initial concentrations of isobutene, ethanol, and 1-butanol. Accordingly, a possible simple kinetic expression based on observed empirical results could be the following:

$$r_i^o = k_i \left(R_{A/IB}^o\right)^{p_{A/IB}} \left(R_{E/B}^o\right)^{p_{E/B}} \quad (7)$$

where $r_i°$ is the initial rate of reaction i, $R°_{A/IB}$ and $R°_{E/B}$ are the initial molar ratios of alcohols-to-isobutene and of ethanol-to-1-butanol, respectively, and they are each raised to the fitted parameters $p_{A/IB}$ and $p_{E/B}$. The factor k_i accounts for an apparent kinetic coefficient for reaction i, which, if an Arrhenius-type temperature dependence is assumed, could take the following form:

$$k_i = \exp\left[k_{1_i} + k_{T_i}\left(1/T - 1/T_m\right)\right] \tag{8}$$

where k_{1_i} and k_{T_i} are the actual fitted parameters, and the mean temperature (T_m) is included to reduce correlation between parameters. Fit of Equation 7 to experimental data is shown in Figure 2.

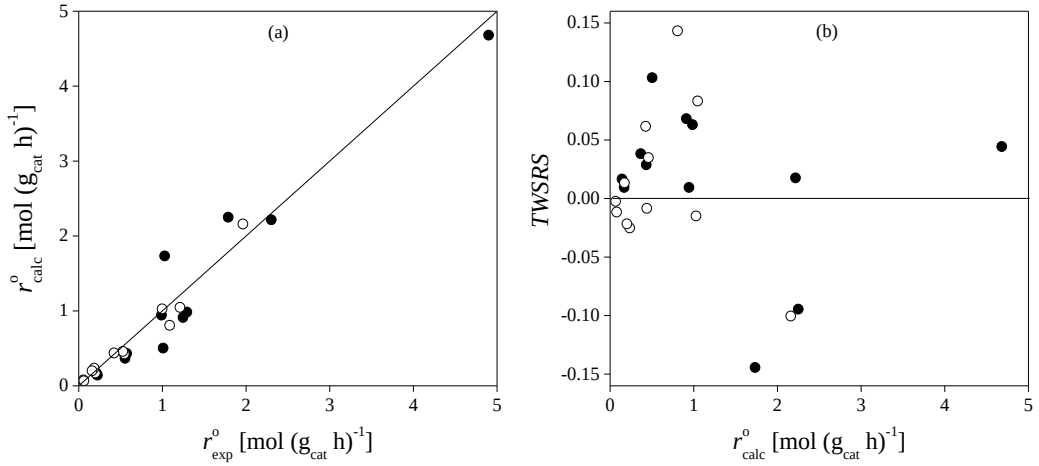

FIGURE 2. Parity plot (a) and residuals distribution (b) for experimental and calculated initial reaction rates with Equation 7 for the syntheses of ETBE (●) and BTBE (○) over A35.

As shown in Figure 2, a rather simple expression like Equation 7 already suffices to describe and predict initial reaction rate data satisfactorily. However, since olefin-ether-alcohols mixtures are highly non-ideal, activities of compounds should be used instead of molar fractions [25]. Furthermore, since the studied reactions are reversible, if reaction rates (r_i) other than the initial ones are to be included in the empirical model, a term related to the progress of each reaction towards the chemical equilibrium can be added to the kinetic model, as follows:

$$r_i = k_i\left(a_{IB}a_{OH} - a_E/K_{eq_i}\right)\left(R^o_{A/IB}\right)^{p_{A/IB}}\left(R^o_{E/B}\right)^{p_{E/B}} \tag{9}$$

where the activity of compound j (a_j) is included (note that the subscripts OH and E in Equation 9 refer, generically, to alcohol and ether, respectively, for every reaction), together with K_{eq_i}, which is the chemical equilibrium constant for either the ETBE or BTBE syntheses, as they were determined in an earlier work [26]:

$$\ln K_{eq_{ETBE}} = \frac{4860}{T} - 11.46 \tag{10}$$

$$\ln K_{eq_{BTBE}} = 870.35 - \frac{105348}{RT} - \frac{1425.42}{R}\ln T + \frac{11.0849}{2R}T - \frac{28.316\times10^{-3}}{6R}T^2 + \frac{2.1305\times10^{-5}}{12R}T^3 \tag{11}$$

It is worth mentioning that the expression used for ETBE equilibrium (Equation 10) is derived from assuming that the reaction enthalpy change can be considered as independent from temperature variations in the explored range, whereas for BTBE (Equation 11) reaction enthalpy change is considered temperature dependent. The choice of equations is consistent with the findings of the quoted work, where BTBE enthalpy of reaction was observed to be more sensitive to temperature variations than ETBE [26].

Needless to say, if more terms are added to the empirical kinetic expression, the fit to experimental rate data can be further improved, provided there is sufficient experimental data. As examples, terms related to the isobutene conversion (X_{IB}), to the activity of the main chemical species (a_j), to the Hildebrand solubility parameter of the reaction medium (δ_M), which has been reported to improve significantly the quality of kinetic fits [27], or combinations of those, can be included. The general empirical expression could be written as follows:

$$r_i = k_i \left(a_{IB} a_{OH} - a_E / K_{eq_i} \right) \prod_m \beta_m^{p_m} \qquad (12)$$

where every β_m term added is raised to its corresponding fitted parameter p_m. Considered $\beta_m^{p_m}$ have been the following: $R°_{A/IB}^{p_{A/IB}}$, $R°_{E/B}^{p_{E/B}}$, $\delta_M^{p_\delta}$, $a_j^{p_j}$, and $(1–X_{IB}^{p_X 2})$. Notice that the fitted parameter associated to the isobutene conversion term (p_X) has been raised to the power 2 to ensure values ranging from zero to unity for that term.

Optimal parameters values of fitted equations, together with their standard errors and the *TWSRS* obtained are listed in Table 2. As seen in the table, some of the added terms include coefficients that are statistically non-significant (that is, the value of their standard error is larger than the parameter value) and, consequently, their inclusion is not justified.

TABLE 2. Optimal parameters values for the fit of Equation 12 to experimental rate data and *TWSRS*. A "—" sign indicates that the related effect is not included in the model.

Mod.	Optimal parameters values											
	$k_{1,ETBE}$	$k_{T,ETBE}\times10^{-3}$	$k_{1,BTBE}$	$k_{T,BTBE}\times10^{-3}$	$p_{A/IB}$	$p_{E/B}$	p_δ	p_X	p_{IB}	p_{EtOH}	p_{BuOH}	*TWSRS*
1	1.2±0.3	-9.9±1.9	0.78±0.13	-8.4±1.1	—	—	—	—	—	—	—	1.188
2	1.26±0.09	-9.6±0.8	0.80±0.07	-8.4±0.6	-0.9±0.2	-0.6±0.2	—	—	—	—	—	0.260
3	1.21±0.12	-10.0±1.2	0.63±0.09	-10.0±0.7	-1.0±0.3	-0.8±0.2	—	7 ± 10^3	—	—	—	0.366
4	1.4±0.9	-9.6±0.8	0.9±0.9	-8.4±0.9	-0.9±0.2	-0.6±0.2	-0.04±0.34	—	—	—	—	0.260
5	1.4±0.9	-9.6±0.8	0.9±0.9	-8.4±0.9	-0.9±0.2	-0.6±0.2	-0.04±0.34	11 ± 10^6	—	—	—	0.260
6	0.5±1.1	-9.1±1.1	0.05±1.1	-7.5±0.6	-1.2±0.2	-0.54±0.14	0.2±0.4	0.78±0.8	-1.6±0.2	—	—	0.210
7	1.8±0.6	-9.9±1.4	1.2±0.6	-9.8±0.6	-0.9±0.2	-0.6±0.2	-0.3±0.2	9 ± 10^4	—	-0.2±0.2	—	0.305
8	1.4±0.9	-10.0±1.9	0.9±0.9	-10.0±0.7	-0.9±0.3	-0.9±0.3	-0.2±0.3	8 ± 10^3	—	—	-0.3±0.4	0.335
9	1.3±1.0	-11.2±0.8	0.9±1.0	-8.8±0.8	-1.4±0.3	-0.7±0.3	-0.2±0.3	0.84±0.11	-1.6±0.3	0.1±0.4	—	0.253
10	0.8±0.9	-10.1±0.8	0.4±0.9	-8.8±0.6	-1.2±0.2	-0.8±0.2	-0.1±0.3	0.85±0.11	-1.5±0.2	—	-0.3±0.4	0.209
11	0.8±1.0	-9.9±0.8	0.4±1.0	-8.5±0.7	-0.8±0.2	-0.6±0.2	0.05±0.30	10 ± 10^5	—	-0.19±0.15	-0.3±0.3	0.235
12	1.2±0.9	-10.0±1.2	0.7±1.0	-10.0±0.7	-1.2±0.3	-1.0±0.4	-0.3±0.3	0.91±0.15	-1.4±0.3	0.1±0.4	-0.4±0.5	0.295

At this point, analysis of the fitting results should be helpful to assessing the effect of every parameter on rates. For instance, according to results, both $R°_{A/IB}$ and $R°_{E/B}$ have a similar effect on rates for the two reactions, since the two parameters are raised to a negative value in all fitted models. Consequently, larger values of $R°_{A/IB}$ and/or $R°_{E/B}$ would reduce observed rates. In this regard, notice that larger values of $R°_{A/IB}$ are related to higher initial concentration of alcohols and, consequently, lower initial concentration of isobutene. As discussed from Figure 1b, lower initial isobutene concentrations would yield lower initial reaction rates, which is consistent with the fitting results. On the other hand, from Figure 1c, larger $R°_{E/B}$ values (that is, higher initial

concentration of ethanol over 1-butanol) should enhance ETBE rates while inhibiting BTBE rates, which is not reflected on the information that can be retrieved regarding $R°_{E/B}$ through the fitting results, probably due to a compensating effect with other variables. Furthermore, the effect on rates of parameters related to the Hildebrand solubility parameter, isobutene conversion, or activity of the main chemical species remains unclear, since some of the optimal values found are positive, some are negative, and some are statistically non-significant.

Therefore, despite being useful tools for predicting rate values (as an example, check the fit of model 2 to experimental data shown in Figure 3), results obtained through empirical fitting procedures are not always informative enough because they are restricted to the interval of the fitted variables, and cannot be relied upon to further understand the physicochemical reality of a reaction system.

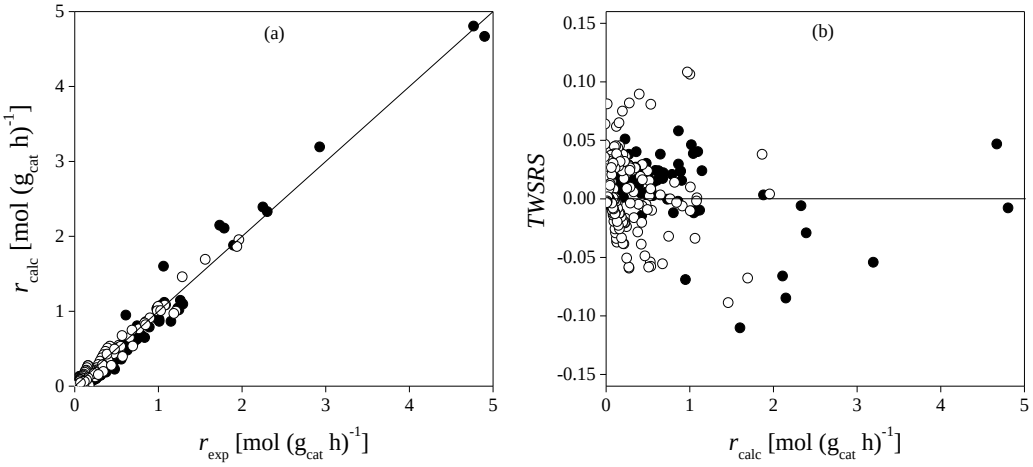

FIGURE 3. Parity plot (a) and residuals distribution (b) for experimental and calculated reaction rates with Equation 12, with optimal parameters of model 2 in Table 2, for the syntheses of ETBE (●) and BTBE (○) over A35.

3.3. MECHANISTIC FIT OF KINETIC DATA

3.3.1. SYSTEMATIC MODELING AND FITTING OF KINETIC DATA

Contrarily to empirical methods, mechanistic kinetic modeling relates rate values with physicochemical properties to establish fundamental relationships that explain observed rate values and allow extrapolations outside the fitted range of the variables. Thus, following the approach of our previous works [16,28], kinetic models were systematically built to include every possible combination of adsorbed and non-adsorbed species in the catalyst active sites, significant and non-significant temperature dependence of parameters, and inclusion or exclusion of a term representing the influence on rates of the interaction between liquid mixture and catalyst particle. General kinetic expression for reaction *i* is as follows:

$$\mathrm{r}_i = \{\text{kinetic term}\}_i \frac{\{\text{driving force}\}_i}{\{\text{adsorption term}\}^{n_i}} \{\text{resin-medium interaction}\} \qquad (13)$$

A detailed description of each term in the general kinetic expression can be found elsewhere [16]. The kinetic terms correspond to apparent kinetic constants (k'_i) and, analogously with Equation 8, they are assumed to follow an Arrhenius-type temperature dependence, as follows:

$$\{\text{kinetic term}\}_i = k_i' = \exp\left[k_{1_i}' + k_{T_i}'\left(1/T - 1/T_m\right)\right] \quad (14)$$

where k'_{1_i} and k'_{T_i} are fitted parameters.

With regards to the driving force terms, it has been assumed that adsorption of reactants and desorption of products would be faster than the surface reaction, which consequently is the rate-determining step for the overall process, as it follows from results in our previous works [16,28] and assumed in many preceding works on similar reaction systems [25,27,29–31]. Therefore, the following expression has been used:

$$\{\text{driving force}\}_i = \left(a_{IB}a_{OH} - \frac{a_E}{K_{eq_i}}\right) \quad (15)$$

where a_j is the activity of compound j and K_{eq_i} is the chemical equilibrium constant for either the ETBE or the BTBE syntheses, which have been shown in Equations 10 and 11.

Regarding the adsorption term, two general forms have been considered, namely Equations 16 and 17:

$$\{\text{adsorption term}\} = 1 + \sum_{\substack{j=\text{EtOH, BuOH,}\\ \text{IB, ETBE, BTBE}}} K_j a_j \quad (16)$$

$$\{\text{adsorption term}\} = a_k + \sum_{j \neq k} K_j a_j \quad (17)$$

Equation 16 corresponds to a situation with a significant fraction of unoccupied active sites on the catalyst surface affecting the reaction rates. Equation 17 derives from assuming that the number of vacant active sites is not significant. In Equations 16 and 17, a_j is the activity of compound j, a_k the activity of compound k, and K_j corresponds either to an adsorption equilibrium constant ($K_j = K_{a,j}$), when the adsorption term has the form of Equation 16, or to a ratio of adsorption equilibrium constants ($K_j = K_{a,j} / K_{a,k}$), when the adsorption term has the form of Equation 17 [16]. The coefficient K_j in both Equation 16 and 17 can be considered as dependent on temperature, or constant within the assayed temperature range. Then, K_j can be expressed either as:

$$K_j = \exp\left[K_{1_j} + K_{T_j}\left(1/T - 1/T_m\right)\right] \quad (18)$$

with $K_{1,j}$ and $K_{T,j}$ as the fitted parameters or, if $K_{T,j}$ is not significant, directly as:

$$K_j = \exp\left(K_{1_j}\right) \quad (19)$$

Since the two reactions take place simultaneously in the same reaction mixture, the adsorption term in their respective kinetic equations should be the same, because of the same relative occupancy of the free and the occupied active sites at a given moment, irrespectively of the reaction considered. The same reasoning applies to the presence or absence of the resin-medium interaction term, which presents the following general equation:

$$\{\text{resin-medium interaction}\} = \exp\left[\frac{\bar{V}_M \phi_P^{\,2}}{RT}\left(\delta_M - \delta_P\right)^2\right] \quad (20)$$

where $\bar{V}_M$ is the molar volume of the liquid mixture, ϕ_P is the catalyst porosity in the swollen-state, R is the gas constant, T is the temperature, and δ_M and δ_P are the Hildebrand solubility parameters of the reaction medium and the catalyst, respectively. If the interaction term is included in the kinetic model, the parameter δ_P can be expressed as follows:

$$\delta_P = k_{P_1} + k_{P_T}\left(T - T_m\right) \quad (21)$$

with k_{P_1} and k_{P_T} as fitting parameters, and T_m being included to reduce total correlation among parameters. If δ_P is not considered as temperature-dependent, k_{P_T} equals zero and, consequently, k_{P_1} is the only fitted parameter.

On the other hand, the exponent in the adsorption term (n_i in Equation 13) can differ between both reactions, since it accounts for the number of active sites, or clusters, involved in each reaction. Values of 1, 2, and 3 have been assumed for every reaction.

Up to 9,504 different equations have been considered in the present kinetic analysis to include all combinations of the aforementioned terms. Table 3 lists the ten best equations obtained according to bias-corrected reduced Akaike Information Criterion (AICc), where optimal parameters values with associated standard errors, *TWSRS*, Δ, and *w* are included.

TABLE 3. Top ten best kinetic equations obtained following a mechanistic approach. A "—" sign indicates that the related effect is not included in the model.

Mod.	k'_{ETBE} (mol/g h)		k'_{ETBE} (mol/g h)		{adsorption term}					n_{ETBE}	n_{BTBE}	δ_P (MPa$^{1/2}$)	*TWSRS*	Δ	*w*
	k'_{ETBE_1}	$k'_{ETBE_T}\times10^{-3}$	k'_{BTBE_1}	$k'_{BTBE_T}\times10^{-3}$	1st Ads[a]	$K_{1_{EtOH}}$	$K_{1_{BuOH}}$	$K_{1_{ETBE}}$	$K_{1_{BTBE}}$			k_{P_1}			
148	-0.7±0.4	-8.4±1.1	-1.2±0.3	-7.4±0.6	a_{EtOH}	—	—	0.4±0.3	—	1	1	27.6±1.9	0.325	0	1.00
4,867	1.0±0.6	-9.5±1.1	1.8±1.0	-8.6±0.7	1	0.8±0.6	—	0.9±0.5	—	1	3	26±2	0.412	40	$<10^{-8}$
200	-0.8±0.5	-8.4±1.2	-1.3±0.4	-7.0±0.7	a_{EtOH}	—	—	—	1.0±0.3	1	1	28±2	0.474	60	$<10^{-13}$
379	0.5±0.2	-9.7±1.2	-0.6±0.3	-8.0±0.8	a_{EtOH}	—	-1.1±0.6	-0.7±0.2	—	1	2	—	0.556	86	$<10^{-18}$
6,740	6±3	-10.0±1.8	7±4	-10.0±1.0	1	2.8±1.4	1.6±0.15	2.1±1.5	—	2	3	—	0.611	103	$<10^{-22}$
6,982	2.4±1.0	-10.0±1.8	2.8±1.2	-10.0±1.1	1	1.4±0.6	—	1. 2±0.5	—	2	3	25±3	0.614	103	$<10^{-22}$
8,855	7±3	-10.0±1.8	6±3	-10.0±1.0	1	2.4±1.1	1.3±1.2	1.8±1.2	—	3	3	—	0.614	103	$<10^{-22}$
1,253	-1.4±0.5	-8.7±1.8	-1.0±0.5	-8.5±0.8	a_{EtOH}	—	—	—	0.5±0.4	2	1	26±3	0.630	105	$<10^{-22}$
1,576	-0.8±0.4	-10±2	-1.4±0.5	-10.0±1.0	a_{EtOH}	—	-1.8±1.0	-0.4±0.3	—	2	2	22±4	0.624	106	$<10^{-23}$
756	0.6±0.2	-9.4±1.5	-1.2±0.3	-7.7±0.8	a_{EtOH}	—	-0.8±0.4	—	-0.3±0.2	1	3	—	0.641	108	$<10^{-23}$

[a] First summand of the adsorption term.

3.3.2. MECHANISTIC MODELING RESULTS

As seen in Table 3, models obtained through the mechanistic approach present similar *TWSRS* values to those from the empirical approach (Table 2) and, consequently, they can be regarded as useful models to predict experimental rate data. On the other hand, among models in Table 3, the best ranked model, namely model 148, is clearly the best fitted model, since it presents a Δ_{148} value of 0 whereas the next best model (i.e., model 4,867) has $\Delta_{4867} = 40$. Previous authors indicated that models can be considered as substantially supported by empirical evidence when they present $\Delta_S < 3$ [20,21].

Besides allowing identification of the most plausible kinetic model (that is, model 148), fitting results listed in Table 3 can also be useful to retrieve some information regarding chemical species adsorption on the catalyst active sites. For instance, within models consistent with assuming that the number of vacant active sites is not significant (that is, those with a_{EtOH} in the first summand of the adsorption term), the ones including the coefficient K_{1BuOH} (namely, models 379, 1576, and 756) show that the relative adsorption of ethanol was greater than that of 1-butanol. For example, for model 379, $K_{1BuOH} = K_{a,BuOH} / K_{a,EtOH} = \exp(-1.1 \pm 0.6) \approx 0.33$, which involves that the ethanol adsorption constant would be about three times greater than the 1-butanol adsorption constant over the assayed experimental conditions. Furthermore, all models consistent with assuming that the number of vacant active sites is significant include $K_{a,EtOH}$ but only one (i.e., model 8855) includes also $K_{a,BuOH}$ and its value is about half that of $K_{a,EtOH}$. These fitting results are consistent with the previously reported preferential adsorption of ethanol over 1-butanol from observation of Fig. 1c. On the other hand, if the same analysis is carried out comparing the adsorption of ethanol with that of both ethers, the fitting results in Table 3 are not that straightforward, since for some models the ethanol adsorption constant would be greater than that of both ethers (e.g., model 6740), but for some others the two produced ethers could be adsorbed in a greater extent than ethanol (e.g., models 148 and 200).

Fit of model 148 to experimental data is shown in Figure 4. As seen, the obtained kinetic equations fit well the experimental kinetic data.

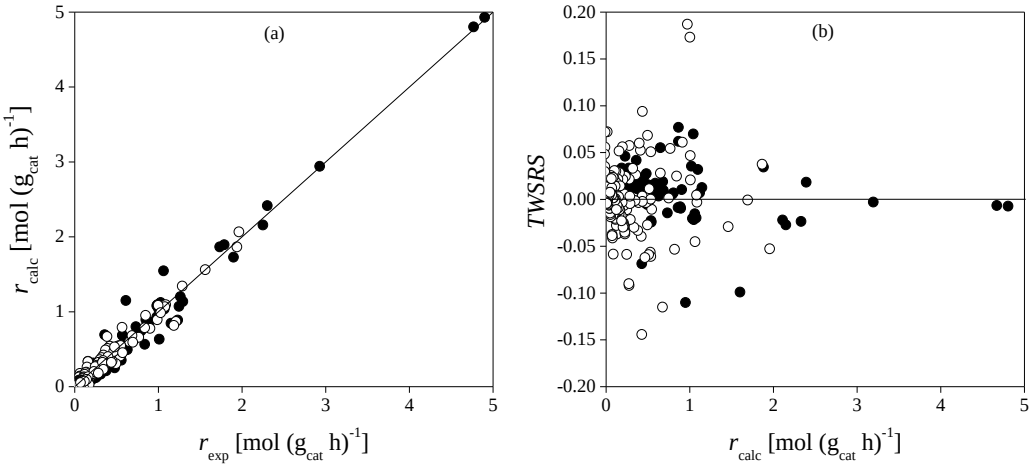

FIGURE 4. Parity plot (a) and residuals distribution (b) for experimental and calculated reaction rates with model 148 for the syntheses of ETBE (●) and BTBE (○) over A35.

For the sake of clarity, the corresponding kinetic equations for each of the reactions taking place in the present system according to model 148 are shown in Equations 22 and 23:

$$r_{ETBE} = exp\left[k'_{ETBE_I} + k'_{ETBE_T}\left(\frac{1}{T} - \frac{1}{333.6}\right)\right] \frac{\left(a_{IB}a_{EtOH} - \frac{a_{ETBE}}{K_{Eq,\,ETBE}}\right)}{a_{EtOH} + exp\left(K_{1_{ETBE}}\right)a_{ETBE}} exp\left[\frac{\bar{V}_M \phi_P^2}{RT}\left(\delta_M - \delta_P\right)^2\right] \qquad (22)$$

$$r_{BTBE} = exp\left[k'_{BTBE_1} + k'_{BTBE_T} \left(\frac{1}{T} - \frac{1}{333.6} \right) \right] \frac{\left(a_{\mathrm{IB}} a_{\mathrm{BuOH}} - \dfrac{a_{\mathrm{BTBE}}}{K_{\mathrm{Eq,\,BTBE}}} \right)}{a_{\mathrm{EtOH}} + exp\left(K_{1_{ETBE}} \right) a_{\mathrm{ETBE}}} exp\left[\frac{\bar{V}_{\mathrm{M}} \phi_{\mathrm{P}}^2}{RT} \left(\delta_{\mathrm{M}} - \delta_{\mathrm{P}} \right)^2 \right] \quad (23)$$

With regards to Equation 23, it might seem counterintuitive that the kinetic equation for the BTBE synthesis does not include 1-butanol in the adsorption term since, obviously, at least one of the reactants must be adsorbed in the resin active sites in order for the reaction to take place in heterogeneous catalysis. Therefore, the fact that 1-butanol is not explicitly included in the adsorption term of model 148 should only be interpreted as it referring to a much lower extension of the adsorption of 1-butanol in comparison to that of ethanol and ETBE. Note that the corresponding term for 1-butanol in model 148 would actually be $K_{1BuOH} = K_{a,BuOH} / K_{a,EtOH}$ and, consequently, if $K_{a,EtOH} >> K_{a,BuOH}$, then $K_{a,BuOH}/K_{a,EtOH} \approx 0$, leading to a quantitatively nonsignificant term. Actually, this fact is consistent with the previously reported preferential adsorption of ethanol over 1-butanol when competing for A35 active sites [11]. The same reasoning could apply for BTBE adsorption.

Equations 22 and 23 cannot be consistent with Langmuir-Hinshelwood-Hougen-Watson (LHHW) mechanisms other than the Eley-Rideal (ER) subtype because the number of involved active sites, or clusters of active sites, is one for the two studied syntheses (that is, $n_{ETBE} = n_{BTBE} = 1$), which inherently avoids the possibility of two molecules being adsorbed in adjacent active sites. Moreover, neither model 148 nor any of the top-ten models in Table 3 include isobutene in the adsorption term. From this, it follows that there is very little evidence that isobutene could be significantly adsorbed on the catalyst active sites. Then, since both reactions occur, it becomes evident that the adsorbed reactant must be the corresponding alcohol rather than isobutene, which must remain in solution.

So, Equations 22 and 23 are consistent with ER mechanisms taking place for both reactions, with the surface reaction step being the rate-determining step of the overall reaction process. Thus, one molecule of the corresponding alcohol, ethanol for the ETBE synthesis and 1-butanol for BTBE, would adsorb on one active site in the resin, or on a single cluster of active sites, whereas the olefin, isobutene, would remain in the liquid phase. Then, one molecule of isobutene from solution and an adsorbed molecule of alcohol would react, giving one adsorbed molecule of the corresponding ether, ETBE or BTBE. Finally, the ether molecule would desorb to the liquid phase. This mechanism is consistent with previous kinetic studies on similar reactions with A35, either for individual reaction systems (e.g., syntheses of MTBE [30], ETBE [29], or PTBE [16]) or simultaneous ones (e.g., ETBE and TAEE [19]).

For every reaction, the kinetic coefficient, k'_i, is related to the actual kinetic constant, k_i, and to adsorption equilibrium constants, $K_{a,j}$. Since n_{ETBE} and n_{BTBE} equal 1, then:

$$k'_{ETBE} = k_{ETBE} \; K_{a,\,\mathrm{EtOH}}^{-(n_{ETBE}-1)} = k_{ETBE} \quad (24)$$

$$k'_{BTBE} = k_{BTBE} \; K_{a,\,\mathrm{EtOH}}^{-n_{BTBE}} K_{a,\,\mathrm{BuOH}} = k_{BTBE} \frac{K_{a,\,\mathrm{BuOH}}}{K_{a,\,\mathrm{EtOH}}} \quad (25)$$

From Equation 24, it follows that the apparent activation energy, E_{ap}, for the ETBE synthesis reaction corresponds to the actual activation energy of the reaction. Then, $E_{\mathrm{ETBE}} = k'_{ETBE_T} \cdot R = (70 \pm 9)$ kJ mol^{-1}, with R being the gas constant. This value is consistent with the one obtained from

the slope of the corresponding line in Figure 1a (i.e., 75 ± 4). On the other hand, from Equation 25, the following relationship can be established between the apparent activation energy ($E_{ap,BTBE}$), the actual activation energy (E_{BTBE}), and the enthalpy changes of adsorption of 1-butanol ($\Delta H°_{a,BuOH}$) and ethanol ($\Delta H°_{a,EtOH}$):

$$E_{ap,BTBE} = E_{BTBE} + \Delta H^{o}_{a,BuOH} - \Delta H^{o}_{a,EtOH} \quad (26)$$

Values of $\Delta H°_{a,BuOH}$ = -(6.9 ± 0.3) kJ mol^{-1} and $\Delta H°_{a,EtOH}$ = -(8.1 ± 0.9) kJ mol^{-1} have been reported in a previous work that studied the adsorption of several compounds on A35 [32]. Thus, E_{BTBE} can be computed from Equation 26 to obtain (60 ± 6) kJ mol^{-1}, which is clearly smaller than the one obtained from the slope of Figure 1a (i.e., 86 ± 6), but close to quoted E_{ap} values for similar reaction systems, typically in the range 67-84 kJ/mol [16,19,22–24].

Parameter K_{ETBE} in the adsorption term corresponds to a ratio of adsorption equilibrium constants, that is, $K_{a,ETBE}/K_{a,EtOH}$. Since K_{ETBE} = 1.5 ± 1.3, the adsorption of ETBE would be slightly stronger than that of ethanol. However, considering the magnitude of the associated uncertainty, it could be stated that the extension of both adsorptions is similar. K_{ETBE} is related to thermodynamic properties of adsorption as follows:

$$\ln K_{ETBE} = \ln \frac{K_{a,ETBE}}{K_{a,EtOH}} = -\frac{\left(\Delta G^{o}_{a,ETBE} - \Delta G^{o}_{a,EtOH}\right)}{RT} = -\frac{\left(\Delta H^{o}_{a,ETBE} - \Delta H^{o}_{a,EtOH}\right)}{R}\frac{1}{T} + \frac{\Delta S^{o}_{a,ETBE} - \Delta S^{o}_{a,EtOH}}{R} \quad (27)$$

where $\Delta G^{o}_{a,j}$, $\Delta H^{o}_{a,j}$ and $\Delta S^{o}_{a,j}$ are the Gibbs free energy, enthalpy and entropy changes of adsorption of compound j, respectively. Since K_{ETBE} is not sensitive to temperature variations, differences in enthalpy and entropy changes of adsorption of ETBE and ethanol on A35 cannot be computed. However, the difference between the Gibbs free energy changes of adsorption of ETBE and ethanol can be obtained, its value being $\Delta G^{o}_{a,ETBE} - \Delta G^{o}_{a,EtOH}$ = -(1.2 ± 0.8) kJ mol^{-1} at 333.6 K. This value suggests that ETBE adsorption on A35 would be slightly more favored than ethanol.

The obtained information regarding the adsorption of ethanol and ETBE on A35, which should be taken carefully, since it has been obtained from the fit of kinetic data, seems to disagree with the scarce available data on individual compounds adsorption on ion-exchange resins. Previous studies have reported stronger adsorption of alcohols (e.g., methanol, ethanol, 1-propanol or 1-butanol) than ethers (e.g., ETBE, MTBE, TAEE or TAME) in the gas-phase [32,33]. Unfortunately, no data has been found regarding the liquid-phase adsorption of these ethers on ion-exchange resins.

Finally, the obtained value of δ_P (27.6 ± 1.9) is very similar to previously reported values for A35, in the range 20.5-24.51 MPa$^{1/2}$ [16,19,28,34], which reinforces the validity of the present results.

3.4. INFORMATION-BASED APPROACH

As seen in previous sections, adopting a systematic approach to build kinetic models for the present reactions system involves building a considerable number of equations, containing a rather high number of adjustable parameters (for instance, there can be up to sixteen fitted parameters in the mechanistic approach, namely k'_{ETBE_1}, k'_{ETBE_T}, k'_{BTBE_1}, k'_{BTBE_T}, K_{IB_1}, K_{IB_T}, K_{EtOH_1}, K_{EtOH_T}, K_{BuOH_1}, K_{BuOH_T}, K_{ETBE_1}, K_{ETBE_T}, K_{BTBE_1}, K_{BTBE_T}, k_{P_1}, and k_{P_T}), and fitting them to experimental data at once. As a matter of fact, except for the chemical equilibrium constants, all other

parameters susceptible of being included in the final kinetic equation, either empirical or mechanistic, have been obtained through the fitting procedure. Given the number of adjustable parameters involved, and considering the implicit complexity of the studied system, it would seem reasonable to suspect that masked effects could be affecting the fitting procedure and model selection thereof.

To check if the modeling results can be regarded as reliable, an alternative approach was adopted to fit the kinetic data, aimed at reducing some of the uncertainty associated to model selection and fitted parameters values. For this approach, previously reported information on the present system (that is, two independent kinetic analyses comprising the present syntheses [19,28] and an adsorption study [32]) was introduced to a kinetic equation that is consistent with the reaction mechanism deduced from the mechanistic kinetic modeling. In particular, all available information on the adsorption of the involved compounds has been used to formulate an adsorption term of the form $a_{\mathrm{EtOH}} + K_{\mathrm{ETBE}}\, a_{\mathrm{ETBE}} + K_{\mathrm{BuOH}}\,(a_{\mathrm{BuOH}} + K_{\mathrm{BTBE}}\, a_{\mathrm{BTBE}})$, with $K_{\mathrm{ETBE}} = K_{a,\mathrm{ETBE}} / K_{a,\mathrm{EtOH}}$, $K_{\mathrm{BuOH}} = K_{a,\mathrm{BuOH}} / K_{a,\mathrm{EtOH}}$ and $K_{\mathrm{BTBE}} = K_{a,\mathrm{BTBE}} / K_{a,\mathrm{BuOH}}$.

Regarding parameters K_{ETBE} and K_{BTBE}, previous kinetic studies [19,28] found the following:

$$K_{\mathrm{ETBE}} = \frac{K_{a,\mathrm{ETBE}}}{K_{a,\mathrm{EtOH}}} = exp\left[-(0.12 \pm 0.04) - (4.6 \pm 0.4)\cdot 10^{3}\left(\frac{1}{T} - \frac{1}{338.4(\mathrm{K})} \right) \right] \tag{28}$$

$$K_{\mathrm{BTBE}} = \frac{K_{a,\mathrm{BTBE}}}{K_{a,\mathrm{BuOH}}} = exp\left[-(1.12 \pm 0.06) - (4.0 \pm 0.3)\cdot 10^{3}\left(\frac{1}{T} - \frac{1}{329.4(\mathrm{K})} \right) \right] \tag{29}$$

Notice that K_{ETBE} values from Equation 28 range from 0.5 at 323 K to 1.6 at 353 K, whereas the value obtained in the present mechanistic fit was 1.5 ± 1.3. The fact that both sources of information produce similar values reinforces their validity.

On the other hand, parameter K_{BuOH} can be deduced from quoted values of thermodynamics of adsorption of ethanol and 1-butanol over A35 in the liquid-phase [32], by taking into account that enthalpy and entropy changes of adsorption (Table 5) are related to adsorption equilibrium constants as follows:

$$ln\, K_{a,j} = -\frac{\Delta H^{o}_{a,j}}{R}\frac{1}{T} + \frac{\Delta S^{o}_{a,j}}{R} \tag{30}$$

TABLE 5. Enthalpy and entropy changes of adsorption of ethanol and 1-butanol over A35 in the liquid phase [32].

Compound	$\Delta H^{o}_{a,j}$ [kJ mol^{-1}]	$\Delta S^{o}_{a,j}$ [J (mol K)$^{-1}$]
Ethanol	-8.1 ± 0.9	-3.7 ± 2.8
1-Butanol	-6.9 ± 0.3	-3.4 ± 1.0

At this point, the kinetic equations that were formulated based on previously reported data and fitted to experimental rates are the following:

$$r_{ETBE} = exp\left[k'_{ETBE_1} + k'_{ETBE_T}\left(\frac{1}{T} - \frac{1}{333.6} \right) \right] \frac{\left(a_{\mathrm{IB}} a_{\mathrm{EtOH}} - \frac{a_{\mathrm{ETBE}}}{K_{\mathrm{Eq}}} \right) exp\left[\frac{\bar{V}_{\mathrm{M}} \phi_{\mathrm{P}}^{2}}{RT} \left(\delta_{\mathrm{M}} - \delta_{\mathrm{P}} \right)^{2} \right]}{a_{\mathrm{EtOH}} + K_{\mathrm{ETBE}} a_{\mathrm{ETBE}} + K_{\mathrm{BuOH}} \left(a_{\mathrm{BuOH}} + K_{\mathrm{BTBE}} a_{\mathrm{BTBE}} \right)} \tag{31}$$

$$r_{BTBE} = exp\left[k'_{BTBE_1} + k'_{BTBE_T} \left(\frac{1}{T} - \frac{1}{333.6} \right) \right] \frac{\left(a_{IB} a_{BuOH} - \frac{a_{BTBE}}{K_{Eq}} \right) exp\left[\frac{\bar{V}_M \phi_P^2}{RT} \left(\delta_M - \delta_P \right)^2 \right]}{a_{EtOH} + K_{ETBE} a_{ETBE} + K_{BuOH} \left(a_{BuOH} + K_{BTBE} a_{BTBE} \right)} \quad (32)$$

where k'_{ETBE_1}, k'_{ETBE_T}, k'_{BTBE_1}, k'_{BTBE_T}, and δ_P are the only fitted parameters, which involves a significant reduction of the total number of adjustable parameters in comparison with previous approaches. Found optimal parameters values and model *TWSRS* are listed in Table 6.

TABLE 6. Optimal parameters values, standard uncertainty, and *TWSRS* of the fit of Equations 31 and 32 to experimental kinetic data.

Coefficient	Optimal value
k'_{ETBE_1}	0.1 ± 0.3
k'_{ETBE_T}	-(9.0 ± 1.3) × 10^3
k'_{BTBE_1}	-(0.4 ± 0.2)
k'_{BTBE_T}	-(8.0 ± 0.7) × 10^3
δ_P	25.5 ± 1.2
TWSRS	0.516

The fit of the present equations to experimental rate data is shown in Figure 5. As seen, despite a somewhat lower quality of the fit if compared to Figures 3 and 4, the present model is able to predict reasonably well all observed rate values. Consequently, the appropriateness of the kinetic mechanism inferred in the present work and the proposed kinetic equations (Equation 22 and 23) is reinforced.

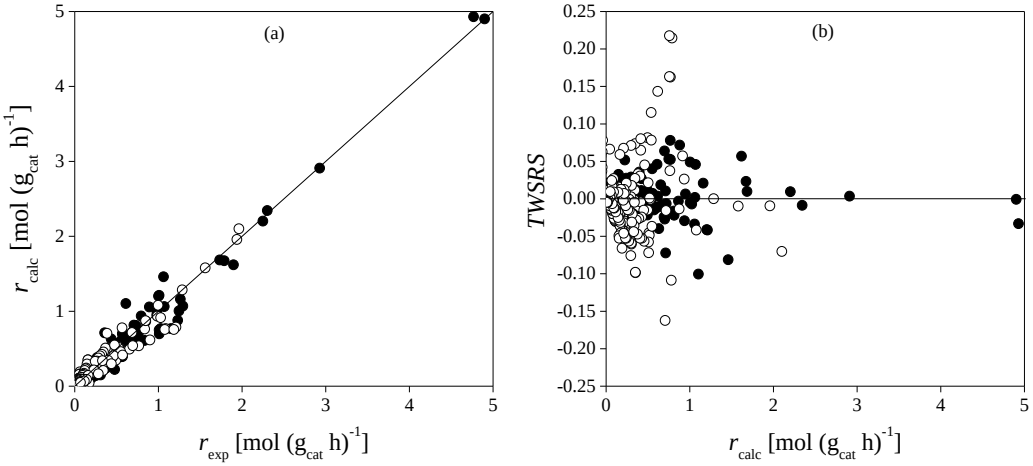

FIGURE 5. Parity plot (a) and residuals distribution (b) for experimental and calculated reaction rates with Equations 31 and 32 for the syntheses of ETBE (●) and BTBE (○) over A35.

4. CONCLUSIONS

The kinetics of the liquid-phase etherification reactions of isobutene with ethanol and with 1-butanol to produce ethyl *tert*-butyl ether (ETBE) and butyl *tert*-butyl ether (BTBE) simultaneously in the same reaction unit over the catalyst Amberlyst™ 35 has been studied in the temperature range of 315 to 353 K. Experimental reaction rates free from mass transfer limitations were used to fit kinetic equations that were built by means of three different approaches, namely empirical, mechanistic, and information-based approach. Empirical kinetic equations produce

optimal quality of the fit, being able to predict kinetic rate data with excellent accuracy using a relatively low number of adjustable parameters and scarce information regarding the operating conditions (e.g., temperature or initial reactants concentration). On the contrary, empirical kinetic equations do not provide enough information to explain the intrinsic nature of the kinetic mechanisms in place. The mechanistic approach provides insight regarding the mechanisms of the studied reactions, as well as information on the compounds adsorption on the catalyst active sites. The best mechanistic kinetic equation for both etherification reactions corresponds to an Eley-Rideal type mechanism in which a molecule of the corresponding alcohol (ethanol or 1-butanol, for ETBE or BTBE synthesis reaction, respectively) is adsorbed on one active site and it reacts with isobutene from solution to produce the adsorbed ether molecule, which finally desorbs. Since the obtained results are consistent with the literature for liquid-phase etherification reactions, an information-based approach can be considered. This approach is based on using previously reported data on the adsorption of the chemical species involved in the present reaction system over the same catalyst and introduce them as variables in reformulated kinetic equations, consistent with the most plausible mechanism. A significant reduction of the total number of adjustable parameters is achieved and the equations fit satisfactorily to all experimental kinetic data. The fact that different sources of information obtained through separate experimental works can be combined and used to obtain consistent results reinforces the validity of the inferred mechanism for the studied reactions system.

Each of the three kinetic fitting approaches present advantages and disadvantages. For instance, the empirical approach is suitable for predicting reaction rate values with maximum accuracy, quickly, and with a manageable amount of variables, albeit restricted to a certain range of operating conditions. The mechanistic approach allows establishing fundamental relationships that can be extrapolated outside the fitted range of the variables, but it involves a considerable computational effort and, potentially, some of the obtained coefficients values should be taken with caution. Finally, the information-based approach can circumvent some of the drawbacks of the mechanistic approach by reducing the number of considered equations and adjustable parameters, but it is only possible when there are enough reported data on the studied system.

LITERATURE

[1] Nanda, S., Rana, R., Vo, D.V.N., Sarangi, P.K., Nguyen, T.D., Dalai, A.K., Kozinski, J.A., 2020. A Spotlight on Butanol and Propanol as Next-Generation Synthetic Fuels, in: Nanda, S., Rana, R., Vo, D.V.N., Sarangi, P.K. (Eds.), Biorefinery of Alternative Resources: Targeting Green Fuels and Platform Chemicals. Springer Singapore, Singapore, 105–126. https://doi.org/10.1007/978-981-15-1804-1_5.

[2] Kulkarni, N. V., Brennessel, W.W., Jones, W.D., 2018. Catalytic Upgrading of Ethanol to n-Butanol via Manganese-Mediated Guerbet Reaction, ACS Catal. 8, 997–1002. https://doi.org/10.1021/acscatal.7b03653.

[3] Cheng, F.L., Guo, H.Q., Cui, J.L., Hou, B., Li, D.B., 2018. Guerbet reaction of methanol and ethanol catalyzed by CuMgAlOx mixed oxides: Effect of M2+/Al3+ ratio, Ranliao Huaxue Xuebao/Journal Fuel Chem. Technol. 46, 1472–1481. https://doi.org/10.1016/s1872-5813(18)30061-6.

[4] Xie, S., Fu, C., Song, W., Zhang, Y., Yi, C., 2019. Highly efficient synthesis and separation of fuel precursors from the concentrated ABE fermentation broth in a biphasic catalytic process, Fuel. 242, 41–49. https://doi.org/10.1016/j.fuel.2019.01.015.

[5] Pinaeva, L., Noskov, A., 2022. Potentials of bio-butanol conversion to valuable products, Rev. Chem. Eng. https://doi.org/10.1515/revce-2021-0066.

[6] Rorrer, J.E., Toste, F.D., Bell, A.T., 2019. Mechanism and Kinetics of Isobutene Formation from Ethanol and Acetone over Zn xZr yO z, ACS Catal. 9, 10588–10604. https://doi.org/10.1021/acscatal.9b03045.

[7] Dagle, R.A., Winkelman, A.D., Ramasamy, K.K., Dagle, V.L., Weber, R.S., 2020. Ethanol as a Renewable Building Block for Fuels and Chemicals, Ind. Eng. Chem. Res. 59, 4843–4853. https://doi.org/10.1021/acs.iecr.9b05729.

[8] Yan, T., Yang, L., Dai, W., Wu, G., Guan, N., Hunger, M., Li, L., 2019. Cascade Conversion of Acetic Acid to Isobutene over Yttrium-Modified Siliceous Beta Zeolites, ACS Catal. 9, 9726–9738. https://doi.org/10.1021/acscatal.9b02850.

[9] Rorrer, J.E., Bell, A.T., Toste, F.D., 2019. Synthesis of Biomass-Derived Ethers for Use as Fuels and Lubricants, ChemSusChem. 12, 2835–2858. https://doi.org/10.1002/cssc.201900535.

[10] Prat, D., Wells, A., Hayler, J., Sneddon, H., McElroy, C.R., Abou-Shehada, S., Dunn, P.J., 2016. CHEM21 selection guide of classical- and less classical-solvents, Green Chem. 18, 288–296. https://doi.org/10.1039/C5GC01008J.

[11] Badia, J.H., Fité, C., Bringué, R., Ramírez, E., Tejero, J., 2017. Simultaneous etherification of isobutene with ethanol and 1-butanol over ion-exchange resins, Appl. Catal. A Gen. 541, 141–150. https://doi.org/10.1016/j.apcata.2017.04.006.

[12] Ancillotti, F., Massi Mauri, M., Pescarollo, E., 1977. Ion exchange resin catalyzed addition of alcohols to olefins, J. Catal. 46, 49–57. https://doi.org/10.1016/0021-9517(77)90134-8.

[13] Ancillotti, F., Massi Mauri, M., Pescarollo, E., Romagnoni, L., 1978. Mechanisms in the reaction between olefins and alcohols catalyzed by ion exchange resins, J. Mol. Catal. 4, 37–48. https://doi.org/10.1016/0304-5102(78)85033-0.

[14] Karinen, R.S., Linnekoski, J.A., Krause, A.O.I., 2001. Etherification of C5- and C8-alkenes with C1- to C4-alcohols, Catal. Letters. 76, 81–87. https://doi.org/10.1023/A:1016788326260.

[15] Casey, W.J., Pietrzyk, D.J., 1973. Nuclear magnetic resonance study of the interaction between cation exchange resins and alcohol and water-alcohol mixtures, Anal. Chem. 45, 1404–1409. https://doi.org/10.1021/ac60330a067.

[16] Badia, J.H., Fité, C., Bringué, R., Iborra, M., Cunill, F., 2019. Systematic kinetic modeling of the propyl *tert*-butyl ether synthesis reaction, Chem. Eng. J. 356, 219–226. https://doi.org/10.1016/j.cej.2018.08.153.

[17] Gates B.C., Rodriguez W., 1973. General and specific acid catalysis in sulfonic acid resin, J. Catal. 31, 27–31. https://doi.org/10.1016/0021-9517(73)90266-2.

[18] Badia, J.H., Fité, C., Bringué, R., Ramírez, E., Iborra, M., 2016. Relevant properties for catalytic activity of sulfonic ion-exchange resins in etherification of isobutene with linear primary alcohols, J. Ind. Eng. Chem. 42, 36–45. https://doi.org/10.1016/j.jiec.2016.07.025.

[19] Soto, R., Fité, C., Ramírez, E., Bringué, R., Cunill, F., 2017. Kinetic modeling of the simultaneous etherification of ethanol with C_4 and C_5 olefins over Amberlyst™ 35 using model averaging, Chem. Eng. J. 307, 122–134. https://doi.org/10.1016/j.cej.2016.08.038.

[20] Symonds, M.R.E., Moussalli, A., 2011. A brief guide to model selection, multimodel inference and model averaging in behavioural ecology using Akaike's information criterion, Behav. Ecol. Sociobiol. 65, 13–21. https://doi.org/10.1007/s00265-010-1037-6.

[21] Burnham, K.P., Anderson, D.R., 2002. Model selection and multimodel inference: a practical information-theoretic approach, 2nd ed., Springer Science & Business Media, New York. https://doi.org/10.1007/b97636.

[22] González, R., Fité, C., Cunill, F., Topp, K.-D., Olsen, R., 2011. Deactivation of Ion Exchange Catalysts by Acetonitrile and Methylamine, Top. Catal. 54, 1054–1062. https://doi.org/10.1007/s11244-011-9725-7.

[23] Santín, Ó., 2005. Estudio del control de las etapas físicas en las síntesis de MTBE y ETBE. MSc thesis. University of Barcelona.

[24] Bozga, G., Motelica, A., Dima, R., Plesu, V., Toma, A., Simion, C., 2008. Evaluation of published kinetic models for *tert*-amyl ethyl ether synthesis, Chem. Eng. Process. Process Intensif. 47, 2247–2255. https://doi.org/10.1016/j.cep.2007.12.002.

[25] Rehfinger, A., Hoffmann, U., 1990. Kinetics of methyl tertiary butyl ether liquid phase synthesis catalyzed by ion exchange resin—I. Intrinsic rate expression in liquid phase activities, Chem. Eng. Sci. 45, 1605–1617. https://doi.org/10.1016/0009-2509(90)80013-5.

[26] Badia, J.H., Fité, C., Bringué, R., Ramírez, E., Cunill, F., 2016. Thermodynamic Analysis of the Experimental Equilibria for the Liquid-Phase Etherification of Isobutene with C_1 to C_4 Linear Primary Alcohols, J. Chem. Eng. Data. 61, 1054–1064. https://doi.org/10.1021/acs.jced.5b00557.

[27] Fité, C., Tejero, J., Iborra, M., Cunill, F., Izquierdo, J.F., 1998. Enhancing MTBE rate equation by considering reaction medium influence, AIChE J. 44, 2273–2279. https://doi.org/10.1002/aic.690441016.

[28] Badia, J.H., Fité, C., Bringué, R., Ramírez, E., Iborra, M., 2021. Liquid-phase synthesis of butyl *tert*-butyl ether catalysed by ion-exchange resins: kinetic modelling through in-depth model discrimination, React. Chem. Eng. 6, 165–172. https://doi.org/10.1039/D0RE00318B.

[29] Fité, C., Iborra, M., Tejero, J., Izquierdo, J.F., Cunill, F., 1994. Kinetics of the Liquid-Phase Synthesis of Ethyl *tert*-Butyl Ether (ETBE), Ind. Eng. Chem. Res. 33, 581–591. https://doi.org/10.1021/ie00027a015.

[30] Parra, D., Tejero, J., Cunill, F., Iborra, M., Izquierdo, J.F., 1994. Kinetic study of MTBE liquid-phase synthesis using C_4 olefinic cut, Chem. Eng. Sci. 49, 4563–4578. https://doi.org/10.1016/S0009-2509(05)80041-7.

[31] Sundmacher, K., Zhang, R.-S., Hoffmann, U., 1995. Mass Transfer Effects on Kinetics of Nonideal Liquid Phase Ethyl *tert*-Butyl Ether Formation, Chem. Eng. Technol. 18, 269–277. https://doi.org/10.1002/ceat.270180408.

[32] Soto, R., Oktar, N., Fité, C., Ramírez, E., Bringué, R., Tejero, J., 2017. Adsorption of C_1-C_4 Alcohols, C_4-C_5 Isoolefins, and their Corresponding Ethers over Amberlyst™35, Chem. Eng. Technol. 40, 889–899. https://doi.org/10.1002/ceat.201600592.

599 [33] Oktar, N., Mürtezaoğlu, K., Doğu, G., Doğu, T., 1999. Dynamic analysis of adsorption
600 equilibrium and rate parameters of reactants and products in MTBE, ETBE and TAME
601 production, Can. J. Chem. Eng. 77, 406–412. https://doi.org/10.1002/cjce.5450770229.

602 [34] González, R., 2011. Performance of Amberlyst™ 35 in the synthesis of ETBE from ethanol
603 and C_4 cuts. PhD Thesis. University of Barcelona.